Stepwise Mechanism for Oxidative Addition of Bromine to Organoselenium(II) and Organotellurium(II) Compounds

Michael R. Detty,*,† Alan E. Friedman,‡ and Martin McMillan§,||

Office Imaging Research and Technical Development, Clinical Diagnostics Research Laboratories, and Analytical Technology Division, Eastman Kodak Company, Rochester, New York 14650

Received April 14, 1994®

The oxidative-addition reactions of bromine (5×10^{-4} or 5×10^{-5} M) to phenyl selenide (**1**), phenyl telluride (**2**), 2,6-di-*tert*-butylselenopyran-4-one (**3**), 2,6-di-*tert*-butyltelluropyran-4-one (**4**), 2,6-diphenyltelluropyran-4-one (**5**), 4-(dicyanomethylidene)-2,6-di-*tert*-butylselenopyran (**6**), and 4-(dicyanomethylidene)-2,6-di-*tert*-butyltelluropyran (**7**), (**1**–**5** at 5×10^{-5} M, **6** and **7** at 1×10^{-5} M) in carbon tetrachloride were monitored by stopped-flow spectroscopy over the temperature range 281.8–307.7 K. Compounds **1**, **2**, **4**, **5**, and **7** gave oxidative-addition products **8**–**12**, while compounds **3** and **6** gave no detectable reaction. Kinetic analysis showed three discrete reactions: an initial fast, second-order (first-order in both bromine and substrate) reaction to give an association complex followed by two consecutive first-order processes to give the final products. Single-crystal, X-ray crystallographic analysis of **14** [from the addition of bromine to 2-((dimethylamino)methyl)phenyl phenyl telluride] was indicative of an ionic structure. The addition of tetra-*n*-butylammonium bromide to **8** and **9** gave the corresponding diphenyl chalcogenides **1** and **2**, respectively, and Br_3^-. Heating crystals of **8** under nitrogen gave melting and gas evolution. The residue was identified as diphenyl selenide (**1**). The data are consistent with multiple, reversible steps in oxidative addition involving entropy-controlled association, ionic dissociation and recombination, and slow conversion of a product mixture of kinetic control to a product mixture of thermodynamic control.

Introduction

In spite of the utility of two-electron changes in the oxidation state of organochalcogen(IV) derivatives,[1-6] little is known about the mechanism of oxidative addition of halogens and pseudohalogens to organoselenium and organotellurium compounds. Recent studies have shown that chlorine and bromine react with telluropyrylium dyes at nearly a diffusion-controlled rate to give tellurium(IV) derivatives.[5] However, reactions with the correpsonding selenopyrylium dyes are slower by 1–2 orders magnitude and the products isolated are from halogenation of the π-framework with no detectable selenium(IV) products. Some mechanistic details may be inferred (through microscopic reversibility) from reductive elimination reactions of tellurium(IV) derivatives, which suggest that discrete steps may be involved in both oxidative addition and reductive elimination.[7] Herein, we describe the observation of at least three distinct steps to oxidative addition of bromine to diorganoselenides and tellurides: an initial, second-order, fast reaction to give bromine complexation followed by consecutively slower, first-order reactions leading to the final oxidative-addition product. The oxidative addition reaction is reversible upon heating and in the presence of added bromide. An ionic tellurium(IV) compound has been characterized as the final product for oxidative addition of bromine to one substrate.

Results and Discussion

Stopped-Flow Kinetics and Spectroscopy. The oxidation of organochalcogen compounds **1**–**7** with bromine in carbon tetrachloride was monitored via stopped-flow spectroscopy. Diphenyl chalcogenides **1** and **2**, telluropyranones **4** and **5**, and telluropyran **7** all gave oxidative-addition products with bromine (**8**–**12**, respectively) with reagent concentrations of 5×10^{-5} to 5×10^{-4} M. Selenopyranone **3** and selenopyran **6** give no apparent reaction with bromine at 293 K at these concentrations. Bromination of the reactive substrates in ethyl acetate, acetone, or acetonitrile gave the same oxidation products although the spectral changes

† Office Imaging Research and Technical Development.
‡ Clinical Diagnostics Research Laboratories.
§ Analytical Technology Division.
|| Author to whom correspondence should be addressed regarding X-ray structural data.
® Abstract published in *Advance ACS Abstracts,* July 1, 1994.

(1) For uses as mild oxidants: (a) Hu, A. X.; Aso, Y.; Otsubo, T.; Ogura, F. *Phosphorus Sulfur* **1988**, *38*, 177. (b) Hu, A. X.; Aso, Y.; Otsubo, T.; Ogura, F. *Tetrahedron Lett.* **1986**, *27*, 6099. (c) Barton, D. H. R.; Finet, J.; Thomas, M. *Tetrahedron* **1986**, *42*, 2319. (d) Barton, D. H. R.; Finet, J.-P.; Giannotti, C.; Thomas, M. *Tetrahedron Lett.* **1988**, *29*, 2671. (e) Detty, M. R.; Luss, H. R. *J. Org. Chem.* **1983**, *48*, 5149. (f) Detty, M. R.; Luss, H. R.; McKelvey, J. M.; Geer, S. M. *J. Org. Chem.* **1986**, *51*, 1692.

(2) As redox catalysts: (a) Ley, S. V.; Meerholz, C. A.; Barton, D. H. R. *Tetrahedron* **1981**, *37*, Suppl. No. 1, 213. (b) Detty, M. R.; Gibson, S. L. *Organometallics* **1992**, *11*, 2147.

(3) In optical recording: Detty, M. R.; Fleming, J. A. *Adv. Mater.* **1994**, *6*, 48.

(4) In chemical storage of solar energy: Detty, M. R.; Gibson, S. L. *J. Am. Chem. Soc.* **1990**, *112*, 4086.

(5) Detty, M. R.; Friedman, A. E. *Organometallics* **1994**, *13*, 533.

(6) As mimics of oxidizing enzymes: (a) Reference 2b. (b) Reference 4. (c) Andersson, C.-M.; Hallberg, A.; Brattsand, R.; Cotgreave, I. A.; Engman, L.; Persson, J. *Bioorg. Med. Chem. Lett.* **1993**, *3*, 2553.

(7) Detty, M. R.; Frade, T. *Organometallics* **1993**, *12*, 2496.

0276-7333/94/2313-3338$04.50/0

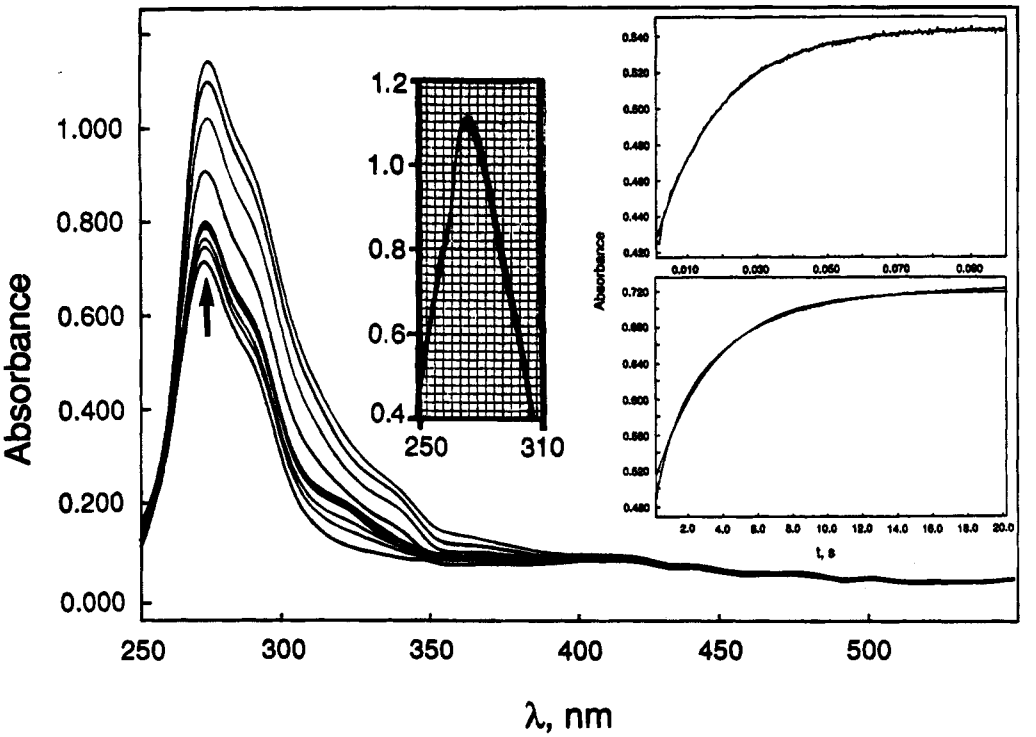

Figure 1. Transient spectra for the oxidative addition of bromine (5×10^{-4} M) to diphenyl selenide (**1**, 5×10^{-5} M) at 281.8 K in carbon tetrachloride. Transient spectra were determined at 0.0015, 0.012, 0.022, 0.0465, 0.079, 0.2, 0.8, 2.0, 4.5, and 15.6 s (traces are sequential from the arrow). The insets show kinetic traces obtained at 290 nm for the fast (upper, pseudo-first-order) and the first "slow" (lower, first-order) reactions at 281.8 K with first-order curve fitting for both processes. The spectral inset shows the isosbestic point (266 nm) observed for the second "slow" reaction over a 20-min time period at 293 K by conventional UV spectroscopy.

associated with bromination in these solvents were not well suited for kinetic analysis.

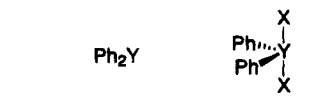

1, Y = Se **8**, Y = Se, X = Br
2, Y = Te **9**, Y = Te, X = Br

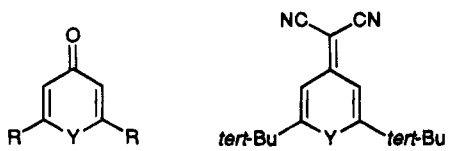

3, R = *tert*-Bu, Y = Se
4, R = *tert*-Bu, Y = Te
5, R = Ph, Y = Te
10, R = *tert*-Bu, Y = $TeBr_2$
11, R = Ph, Y = $TeBr_2$

6, Y = Se
7, Y = Te
12, Y = $TeBr_2$

The products of bromine oxidation have all been characterized in the literature. The X-ray crystal structures of bromine oxidative-addition products **8**[8] and **9**[9] have been described. The bromine oxidative-addition products of **4**, **5**, and **7** (**10**–**12**, respectively) have been isolated and characterized spectroscopically,[10] and an X-ray structure of a derivative of **10** has been described.[11] *trans*-Diaxial bromide ligands in a trigonal-bipyramidal array with the metal atom lone pair of electrons stereochemically active were observed in all three X-ray structures. The products formed in the kinetics experiments were spectroscopically identical to materials formed in preparative runs.

In the reaction of diphenyl selenide (**1**) with bromine, three kinetically distinct processes were observed at 281.8 and 289.4 K. Transient spectra for the oxidative addition of bromine to **1** at 281.8 K are shown in Figure 1. The insets of Figure 1 show kinetic traces and their best first-order fit at 290 nm for two different reactions observed in the transient spectra. A third, slower process was also observed. This process was best followed by conventional spectroscopic techniques. Although spectral changes were much smaller for the slowest process, an isosbestic point was observed at 266 nm at 293 K (spectral inset of Figure 1). At temperatures above 290 K, only the initial fast reaction and the final slow reaction could be separated from other processes. Rate constants for these processes at several temperatures are compiled in Table 1.

The fast process in the oxidative addition of bromine (5×10^{-5} M) to diphenyl telluride (**2**, 5×10^{-5} M) in carbon tetrachloride approached diffusion control at 283.7 K with a half-life of ≤ 0.3 ms ($k \geq 5 \times 10^8$ L mol^{-1} s^{-1}). While a slower process was observable, the spectral changes associated with this reaction were too small for accurate rate constants to be determined although a first-order rate constant would be in the 10^{-1} to 10^{-2} s^{-1} range.

(8) McCullough, J. D.; Hamburger, G. *J. Am. Chem. Soc.* **1941**, *63*, 803.
(9) Christofferson, G. D.; McCullough, J. D. *Acta Crystallogr.* **1958**, *11*, 249.
(10) Detty, M. R.; Murray, B. J. *J. Org. Chem.* **1987**, *52*, 2123.
(11) Detty, M. R.; Luss, H. R. *Organometallics* **1986**, *5*, 2250.

Table 1. Observed Rates and Calculated Rate Constants for Oxidative Addition of Bromine (5×10^{-4} M) to Diorganochalcogenides 1, 2, 4, and 5 at 5×10^{-5} M and 7 at 1×10^{-5} M in CCl_4

compd	T, ±0.1 K	k_{obs}(fast), s^{-1}	k(fast),[a] L Mol^{-1} s^{-1}	k_{obs}(2nd),[b] s^{-1}	k_{obs}(slow),[b] s^{-1}	λ_{meas}, nm
1	281.8	2.12 ± 0.02	4.24×10^3	$(4.35 \pm 0.07) \times 10^{-1}$	$(2.27 \pm 0.21) \times 10^{-3}$	290
	283.7	0.201 ± 0.002[c]	4.02×10^3	$(4.41 \pm 0.11) \times 10^{-1}$	$(2.41 \pm 0.13) \times 10^{-3}$	
	283.7	1.90 ± 0.02	3.80×10^3	$(4.38 \pm 0.07) \times 10^{-1}$	$(2.36 \pm 0.07) \times 10^{-3}$	
	289.7	1.77 ± 0.02	3.54×10^3	$(5.61 \pm 0.11) \times 10^{-1}$	$(2.76 \pm 0.06) \times 10^{-3}$	
	294.3	1.66 ± 0.01	3.33×10^3		$(4.41 \pm 0.30) \times 10^{-3}$	
	300.8	1.47 ± 0.01	2.94×10^3		$(5.49 \pm 0.39) \times 10^{-3}$	
	306.7	1.42 ± 0.02	2.84×10^3		$(7.12 \pm 0.19) \times 10^{-3}$	
2	283.7	$\geq 10^4$[c]	$\geq 2 \times 10^8$		10^{-1}–10^{-2}	300
4	289.3	5.70 ± 0.10	1.14×10^4			300
	290.3	0.453 ± 0.02[c]	9.06×10^3			
	297.7	6.00 ± 0.09	1.20×10^4			
	307.7	6.40 ± 0.3	1.28×10^4			
5	283.5	2.385 ± 0.016	4.79×10^3		$(2.28 \pm 0.03) \times 10^{-2}$	370
	289.3	2.37 ± 0.03	4.74×10^3		$(2.88 \pm 0.04) \times 10^{-2}$	
	294.0	2.15 ± 0.04	4.30×10^3		$(3.57 \pm 0.04) \times 10^{-2}$	
	298.7	1.815 ± 0.009	3.63×10^3			
	303.3	1.84 ± 0.07	3.68×10^3			
7	283.7	1.23 ± 0.02	2.46×10^3	$(3.81 \pm 0.04) \times 10^{-2}$	$(2.02 \pm 0.02) \times 10^{-3}$	370
	289.7	1.30 ± 0.02	2.60×10^3	$(4.8 \pm 0.3) \times 10^{-2}$	$(2.76 \pm 0.07) \times 10^{-3}$	
	294.3	1.27 ± 0.01	2.54×10^3		$(3.97 \pm 0.13) \times 10^{-3}$	
	300.4	1.17 ± 0.08	2.34×10^3		$(4.37 \pm 0.11) \times 10^{-3}$	
	303.0	1.123 ± 0.006	2.25×10^3	$(2.0 \pm 0.3) \times 10^{-1}$		

[a] k_{obs} divided by $[Br_2]$. [b] From first-order curve fitting. [c] Second-order curve fitting with stoichiometric bromine (5×10^{-5} M).

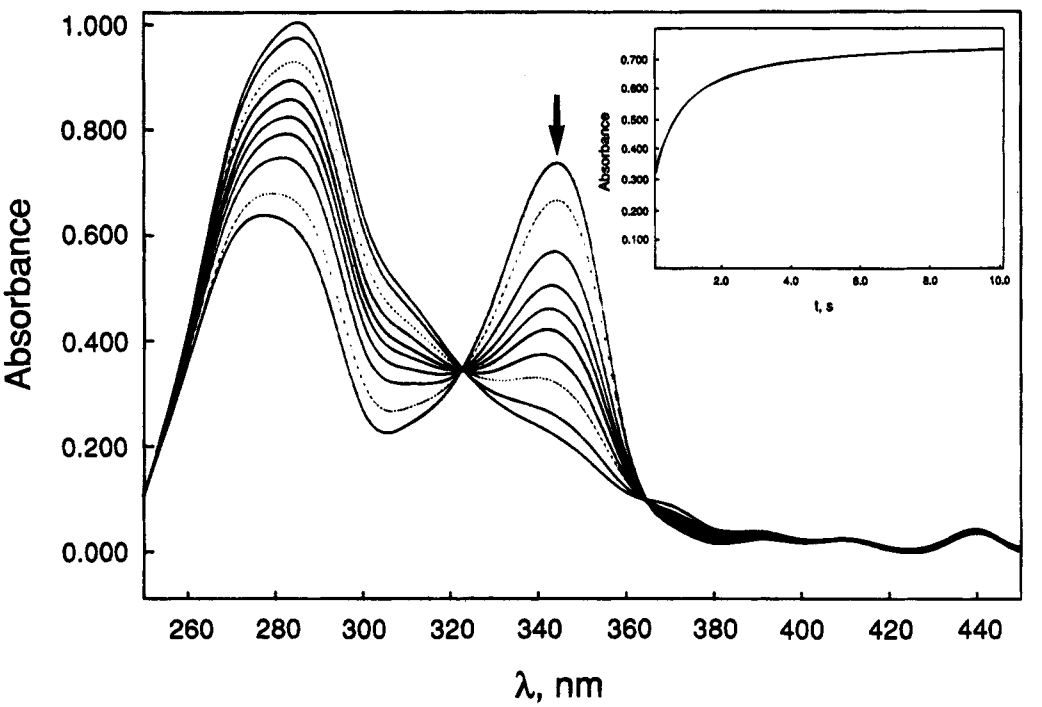

Figure 2. Transient spectra for the fast reaction for oxidative addition of bromine (5×10^{-5} M) to telluropyranone **4** (5×10^{-5} M) at 297.7 K in carbon tetrachloride. Transient spectra were determined at 0.05, 0.125, 0.275, 0.425, 0.575, 0.75, 1.08, 1.60, 3.48, and 9.55 s (traces are sequential from the arrow). The inset shows a kinetic trace obtained at 300 nm for the fast reaction at 297.7 K with second-order curve fitting.

The fast process in the oxidative addition of bromine (5×10^{-5} M) to telluropyranone **4** (5×10^{-5} M) followed beautiful isosbestic behavior in the transient spectra of Figure 2, while a kinetic trace at 300 nm gave an excellent second-order fit (inset of Figure 2). Again, a slower process was observable but spectral changes were too small for meaningful kinetic analysis.

For the oxidative addition of bromine (5×10^{-4} M) to tellurapyranone **5** (5×10^{-5} M), a fast reaction and a slow reaction were observed between 283.5 and 294.0 K. At higher temperatures, spectral changes were much smaller for the slow reaction and only the fast reaction could be separated.

For telluropyran **7**, three kinetically distinct processes were observed at 370 nm at 283.7, 289.7, and 303 K. At temperatures of 294.3 and 300.4 K, only the initial fast reaction and the final slow reaction could be resolved. An isosbestic point was observed at 395 nm for the middle process, as shown in Figure 3 at 303 K.

Activation Parameters. The initial, fast reaction in each of these systems was found to follow second-order kinetic behavior with the second-order rate constant having a first-order dependence on both bromine and the organochalcogen compound. Calculated second-order rate constants from either pseudo-first-order

Scheme 1

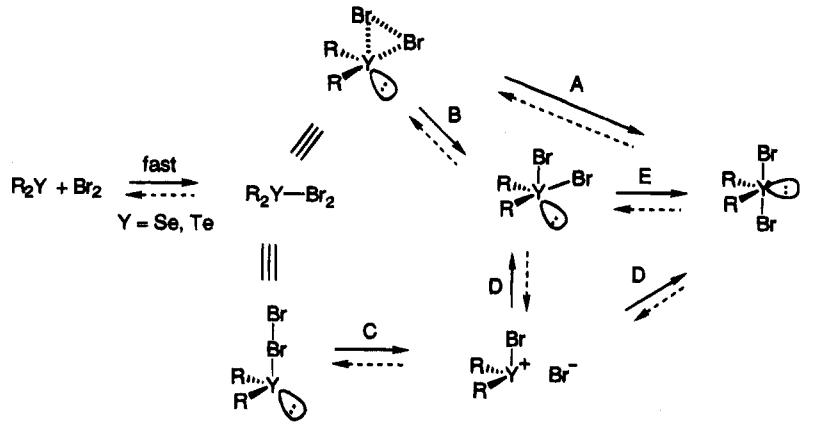

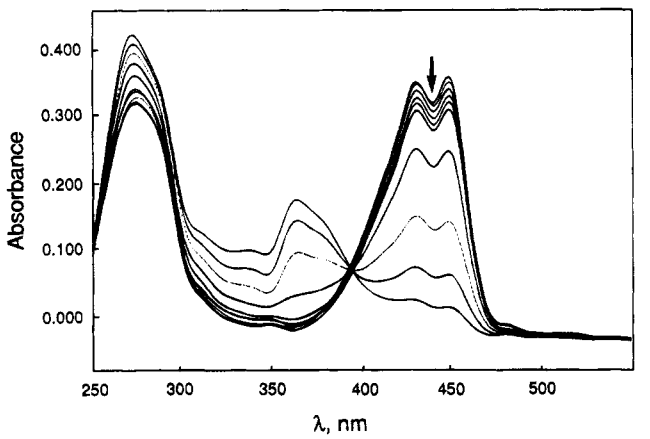

Figure 3. Transient spectra for the oxidative addition of bromine (5×10^{-4} M) to telluropyran **7** (1×10^{-5} M) in carbon tetrachloride at 303 K illustrating the "fast" and "middle" reactions. Transient spectra were determined at 0.025, 0.035, 0.05, 0.11, 0.2875, 0.500, 1.653, 3.903, 6.753, and 10.45 s (traces are sequential from the arrow). An isosbestic point is observed at 395 nm for the middle reaction.

conditions or second-order curve fitting were nearly identical (Table 1).

From the rate constants, Arrhenius and Eyring activation parameters were calculated and are compiled in Table 2. Values of E_a and $\Delta H^{\ddagger}$ are near 0 kcal mol^{-1} for all four systems in which temperature dependence could be measured. Consequently, barriers to reaction must be entropic in nature and are reflected in large, negative values of $\Delta S^{\ddagger}$. The fast reactions of **1**, **5**, and **7** with bromine actually show inverted Arrhenius behavior with small, negative values of E_a (Table 2). Values of $\Delta G_{298}^{\ddagger}$ are calculated to be 12.3 kcal mol^{-1} for **1**, 11.8 kcal mol^{-1} for **4**, 12.5 kcal mol^{-1} for **5**, and 12.8 kcal mol^{-1} for **7**.

The fast reaction was followed by two slower reactions, which displayed first-order rate behavior (Table 1). The rate constants for these reactions were independent of both substrate and bromine concentration. The middle reaction was observed over too small a temperature range to calculate accurate activation parameters for **1**. However, for **7** E_a is 15.2 kcal mol^{-1} and $\Delta H^{\ddagger}$ is 14.6 kcal mol^{-1} while $\Delta S^{\ddagger}$ is −13 cal mol^{-1} K^{-1}. For the slowest reaction, values of E_a and $\Delta H^{\ddagger}$ fall between 6.5 and 8.9 kcal mol^{-1} while values of $\Delta S^{\ddagger}$ are between −41 and −43 cal mol^{-1} K^{-1} (Table 2). The corresponding calculated values of $\Delta G_{298}^{\ddagger}$ are 20.5, 19.3, and 20.5 kcal mol^{-1} for **1**, **5**, and **7**, respectively. Barriers to the reaction for the slowest step have a large entropic contribution.

Mechanistic Considerations. The kinetically distinct pathways suggest that oxidative-addition reactions occur in discrete steps. Presumably, the fast reaction is an initial association of bromine with the heteroatom, as shown in Scheme 1, perhaps a charge-transfer type of interaction in view of the small activation barriers to reaction. The charge-transfer complex could involve either an η^1-complex (end-on approach) or an η^2-complex (edge-on approach). An X-ray crystal structure of the iodine-1,4-diselenahexane charge-transfer complex, which does not react to give oxidative-addition products, shows an axial, η^1-complex of I_2 with the selenium atoms.[12] The rate of the fast reaction appears to be associated with electron density at the heteroatom. In the organotellurium series, the fast reaction becomes slower as the organic ligands become more electron withdrawing with k(fast) decreasing in the order **2** > **4** > **5** > **7**. In the organoselenium series, the fast reaction is only observed with **1**, which has the most electron-rich Se center of this study. The more electron-deficient members of the series do not give a detectable reaction under our conditions of reaction.

Our speculation on possible steps in the mechanism of oxidative addition are also shown in Scheme 1. From the initial association complex, concerted oxidative addition across an edge of the η^2-complex (the faster "slow" reaction) might lead directly to the final product via path A, to *cis*-dibromide ligands as in path B, or to a mixture of *cis*- and *trans*-dibromides. Alternatively, a dissociative mechanism from the η^1-complex as shown in path C would lead to ionic intermediates, which could then collapse to the *trans*-diaxial and/or *cis*-chalcogen-(IV) dibromides. Pseudorotation could interconvert the *cis*- and *trans*-dibromides via path E, as could dissociation along path D to give a thermodynamic product mixture from a kinetic product mixture (the slower "slow" reaction). Thermal reductive elimination reactions of chloride or bromine from other Te(IV) derivatives suggest that the steps involved in oxidative addition are chemically reversible.[3,7]

(12) McCullough, J. D.; Chao, G. Y.; Zuccaro, D. E. *Acta Crystallogr.* **1959**, *12*, 815.

Table 2. Arrhenius and Eyring Activation Parameters for the Fast and Slow Reactions in the Oxidative Addition of Bromine to Diorganochalcogenides 1, 4, 5, and 7 in CCl_4[a]

compd	reacn	E_a, kcal mol^{-1}	ln A	$\Delta H^{\ddagger}$, kcal mol^{-1}	$\Delta S^{\ddagger}$, cal mol^{-1} K^{-1}	$\Delta G_{298}^{\ddagger}$, kcal mol^{-1}
1	fast	-2.6 ± 0.5	4 ± 2	-3.2 ± 0.5	-52 ± 4	12.3
	slow	8.3 ± 1.5	9 ± 2	7.7 ± 1.5	-43 ± 7	20.5
4	fast	1.1 ± 0.1	11.3 ± 0.5	0.5 ± 0.1	-38 ± 1	11.8
5	fast	-2.7 ± 1.2	3.7 ± 0.4	-3.3 ± 1.1	-53 ± 6	12.5
	slow[b]	7.06 ± 0.02	8.7 ± 0.1	6.50 ± 0.09	-43 ± 1	19.3
7	fast	-0.9 ± 1.1	6 ± 1	-1.5 ± 1.1	-48 ± 5	12.8
	middle	15.2 ± 0.2	23.4 ± 1.4	14.6 ± 0.2	-13 ± 3	18.5
	slow	8.9 ± 2.4	10 ± 2	8.3 ± 2.4	-41 ± 6	20.5

[a] Errors given are $\pm 2\sigma$. For the fast reactions, only data determined under pseudo-first-order conditions were employed. [b] These small error values are fortuitous.

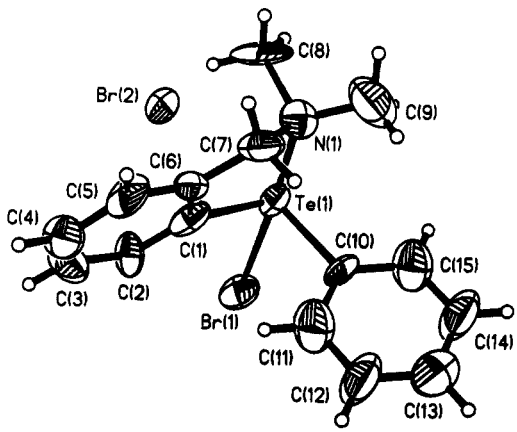

Figure 4. ORTEP drawing with thermal ellipsoids shown at the 50% probability level and the numbering scheme for the crystal structure of **14**.

Ionic Intermediates and *cis*-Bromines along the Reaction Path. Diaryl telluride **13** has an *o*-[(dimethylamino)methyl] substituent, which is capable of stabilizing an ionic intermediate. In structure **14**, the

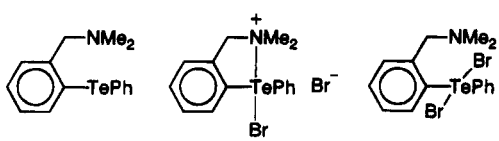

13 **14** **15**

lone pair of electrons on nitrogen can stabilize an ionic intermediate by functioning as a neutral donor ligand *trans* to the bromide at Te(IV). Alternatively, *trans*-diaxial (**15**) or *cis* addition of bromine is still possible to give nonionic complexes in which the lone pair of electrons on nitrogen is coordinated to an octahedral site.

The addition of bromine to an acetone solution of **13** gave gold crystals marginally suitable for X-ray crystallographic analysis. The refined structure was indicative of the ionic structure **14** although the R_1 value was high. (The crystal structure analysis was repeated on a crystal selected from a group of crystals grown from carbon tetrachloride, and a comparable data set was obtained.) An ORTEP drawing of **14** showing thermal ellipsoids at the 50% probability level and the numbering scheme for the molecule are presented in Figure 4. Crystal data are given in Table 3, bond lengths and angles are given in Table 4, and atomic coordinates and equivalent isotropic displacement parameters are given in Table 5. Anisotropic displacement parameters and hydrogen coordinates with isotropic displacement parameters are found in Tables 7 and 8, respectively, which are found in the supplementary material.

Table 3. Crystal Data and Structure Refinement for Bromo[2-((dimethylamino)methyl)phenyl]phenyltelluronium Bromide (14)

empirical formula	$C_{15}H_{17}Br_2NTe$
fw	498.72
temp (K)	293(2)
wavelength (Å)	0.710 73
cryst syst	triclinic
space group	$P\bar{1}$
unit cell dimens	
a (Å)	9.515(5)
b (Å)	9.744(5)
c (Å)	11.634(10)
α (deg)	92.11(6)
β (deg)	106.01(6)
γ (deg)	114.97(6)
vol (Å^3)	925.2(10)
Z	2
density (calcd) (g/cm^3)	1.790
abs coeff (mm^{-1})	5.915
F(000)	472
cryst size (mm)	0.2 × 0.4 × 0.4
θ range for data collcn (deg)	3.70–26.35
index ranges	$-13 \le h \le 12$, $-13 \le k \le 13$, $0 \le l \le 16$
no. of ind reflns	3454
refinement method	full-matrix least squares on F^2
data/restraints/params	3454/0/150
goodness-of-fit on F^2	1.146
final R indices [$I > 2\sigma(I)$]	$R_1 = 0.1007$, $wR_2 = 0.2539$
R indices (all data)	$R_1 = 0.1331$, $wR_2 = 0.3285$
largest diff peak and hole (e Å^{-3})	+2.418 and −3.910

The geometry about the Te atom in **14** is a distorted octahedron with Br1, Br2, C1, C10, N, and a stereochemically active lone pair of electrons occupying the octahedral sites. The C1—Te—C10 angle is 92.3°, and the N—Te—Br1 angle is 168.8°. In the latter angle, the distortion from linearity is due in part to the constraint of the five-membered ring, which is formed upon chelation, and in part to Te lone-pair stereochemical activity. The Br1—Te···Br2, Br1—Te—C1, and Br1—Te—C10 angles are all nearly right angles as are the N—Te—C1, N—Te—C10, and N—Te···Br2 angles (Table 4). To complete the octahedron, the C10—Te···Br2 angle is nearly linear at 173.5°. This geometry can be contrasted with the geometry about the Te atom of **9**, which is trigonal bipyramidal.[9]

The Te—Br1 bond length of 2.632 Å is typical of "hypervalent" Te—Br bonds when compared to Te—Br bond lengths in **16** (2.682 Å)[11] and **17** (2.644 Å).[1e] However, the Te···Br2 distance is much longer at 3.402 Å, which is just under the sum of van der Waals' radii for the two atoms (3.91 Å).[13] While Br^- is located near the Te atom, the bonding interaction is quite weak and is mostly ionic. The two bromine atoms are found in a *cis* geometry around the Te atom in this molecule, which

(13) Bondi, A. *J. Phys. Chem.* **1964**, *68*, 441.

Table 4. Bond Lengths (Å) and Angles (deg) for 14

	Bond Lengths		
Te1—C1	2.110(14)	C6—C7	1.52(2)
Te1—C10	2.140(8)	C7—N1	1.49(2)
Te1—N1	2.389(12)	N1—C9	1.41(3)
Te1—Br1	2.632(2)	N1—C8	1.49(2)
Te1—Br2	3.402(4)	C10—C11	1.39
C1—C6	1.39(2)	C10—C15	1.39
C1—C2	1.42(2)	C11—C12	1.39
C2—C3	1.37(2)	C12—C13	1.39
C3—C4	1.34(3)	C13—C14	1.39
C4—C5	1.44(3)	C14—C15	1.39
C5—C6	1.40(2)		
	Bond Angles		
C1—Te1—C10	92.3(5)	C1—C6—C7	121.3(14)
C1—Te1—N1	76.7(6)	C5—C6—C7	121(2)
C10—Te1—N1	84.8(5)	N1—C7—C6	108.5(14)
C10—Te1—Br1	93.4(4)	C9—N1—C8	107(2)
C10—Te1—Br1	90.5(4)	C9—N1—C7	115(2)
N1—Te1—Br1	168.8(3)	C8—N1—C7	108.2(14)
C1—Te1—Br2	81.7(4)	C9—N1—Te1	114.3(14)
C10—Te1—Br2	173.5(3)	C8—N1—Te1	104.0(9)
N1—Te1—Br2	96.1(3)	C7—N1—Te1	107.5(9)
Br1—Te1—Br2	87.55(8)	C11—C10—C15	120.0
C6—C1—C2	119.8(12)	C11—C10—Te1	120.3(6)
C6—C1—Te1	116.1(12)	C15—C10—Te1	119.7(6)
C2—C1—Te1	123.8(10)	C12—C11—C10	120.0
C3—C2—C1	121(2)	C11—C12—C13	120.0
C4—C3—C2	121(2)	C12—C13—C14	120.0
C3—C4—C5	119(2)	C15—C14—C13	120.0
C6—C5—C4	121(2)	C14—C15—C10	120.0
C1—C6—C5	117.7(14)		

Table 5. Atomic Coordinates and Equivalent Isotropic Displacement Parameters (Å²) for 14

atom	*x*	*y*	*z*	U_{eq}[a]
Te1	0.2313(1)	0.6381(1)	0.1649(1)	0.044(1)
Br1	0.1870(2)	0.8869(2)	0.1534(2)	0.062(1)
Br2	0.1722(2)	0.6071(2)	−0.1388(1)	0.061(1)
C1	0.4785(16)	0.7559(20)	0.1727(12)	0.048(4)
C2	0.5461(17)	0.8991(20)	0.1346(16)	0.056(4)
C3	0.7046(21)	0.9644(20)	0.1332(19)	0.067(5)
C4	0.8022(20)	0.8974(20)	0.1730(18)	0.061(4)
C5	0.7360(20)	0.7509(22)	0.2110(17)	0.061(4)
C6	0.5726(16)	0.6779(15)	0.2074(12)	0.040(3)
C7	0.5070(25)	0.5279(18)	0.2541(16)	0.064(5)
N1	0.3258(17)	0.4466(15)	0.1961(12)	0.051(3)
C8	0.2894(24)	0.3703(21)	0.0706(19)	0.077(6)
C9	0.2418(35)	0.3318(24)	0.2560(26)	0.097(8)
C10	0.2948(14)	0.6793(14)	0.3586(7)	0.053(4)
C11	0.4427(13)	0.8005(15)	0.4286(9)	0.080(4)
C12	0.4803(13)	0.8308(15)	0.5539(9)	0.092(5)
C13	0.3697(17)	0.7399(17)	0.6092(7)	0.078(5)
C14	0.2218(16)	0.6187(16)	0.5392(10)	0.092(5)
C15	0.1843(13)	0.5884(14)	0.4139(10)	0.080(4)

[a] U_{eq} is defined as one-third of the trace of the orthogonalized U_{ij} tensor.

has not been observed in other Te(IV) derivatives. The Te—N bond length of 2.389 Å is somewhat longer than the 2.02–2.11-Å Te—N bond lengths found in several 1,2-tellurazoles[14] and 1,2,5-telluradiazoles[15] but is much less than the sum of van der Waals' radii for the two atoms (3.61 Å).[13]

Effects of Added Bromide. The addition of incremental amounts of tetra-*n*-butylammonium bromide to a $CDCl_3$ solution of **8** gave increasing concentrations of diphenyl selenide (**1**), as detected by ^1H NMR as shown in Figure 5. Presumably, the presence of bromide leads to the formation of Br_3^- and diphenyl selenide (**1**) from **8**. Similar results were obtained upon the addition of incremental amounts of tetra-*n*-butylammonium bromide to a $CDCl_3$ solution of **9**, which showed the chemical shifts of the protons of **9** "moving" toward those of the protons of **2** although more bromide was required to affect the same changes as observed with **8**. These data suggest that the many steps of the oxidative addition are reversible and that the presence of added bromide disrupts the equilibrium by capturing free bromine as tribromide. The equilibria of Scheme 1 lie further to the right with diphenyl telluride (**2**) than with diphenyl selenide (**1**).

To our knowledge, the equilibrium constant for the addition of bromide to bromine to give tribromide (eq 1) in carbon tetrachloride or chlorform has not been reported in the literature. If the equilibrium constant

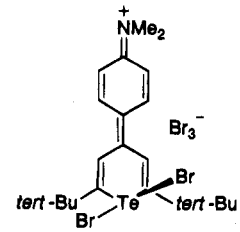

16

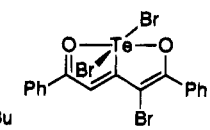

17

were similar to that reported for the addition of iodide to iodine to give triiodide ($\approx 10^3$ M^{-1}),[16] then one can estimate the equilibrium constants for diphenyl selenide (**1**) plus bromine to give diphenylselenium(IV) dibromide (**8**, eq 2). The addition of 0.015 M tetra-*n*-butylammonium bromide to 0.01 M **8** in deuteriochloroform gave an ^1H NMR spectrum whose chemical shift for the *ortho* protons was halfway between the chemical shifts for the *ortho* protons of pure **1** and **8**. If one assumes a concentration of 0.005 M in both **1** and **8** at this point and a K_{eq} of 10^3 M^{-1} for the tribromide equilibrium, then the concentration of free bromine is $\approx 5 \times 10^{-4}$ M and K_{eq} for eq 2 is $\approx 2 \times 10^3$ M^{-1} at 293 K.

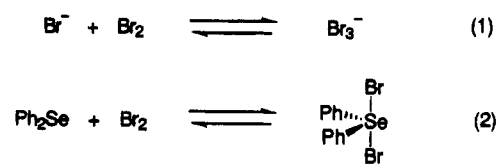

Thermal Reductive Elimination of Bromine from 8. When crystals of **8** are heated to 200 °C under a stream of nitrogen, melting and gas evolution are observed. After 30 min of heating, cooling to ambient temperature yields a yellow oil, which was identified as diphenyl selenide (**1**) by its ^1H NMR spectrum. These data suggest that oxidative addition of bromine to **1** is reversible and is an equilibrium process.

Summary and Conclusions

The oxidative addition of bromine to organoselenium(II) and organotellurium(II) compounds appears to involve multiple steps and the fast, initial step of oxidative addition is affected by the electronic environment of the chalcogen. Electron-deficient Se centers as

(14) (a) DeMunno, G.; Lucchesini, F. *Acta Crystallogr., Sect. C: Cryst. Struct. Commun.* **1992**, *C48*, 1437. (b) Campsteyn, H.; Dupont, L.; Lamotte-Brasseur, J.; Vermeire, M. *J. Heterocycl. Chem.* **1978**, *15*, 745.

(15) Bertini, V.; Dapporto, P.; Lucchesini, F.; Sega, A.; DeMunno, A. *Acta Crystallogr., Sect. C: Cryst. Struct. Commun.* **1984**, *40C*, 653.

(16) Watts, H. *Aust. J. Chem.* **1961**, *14*, 15.

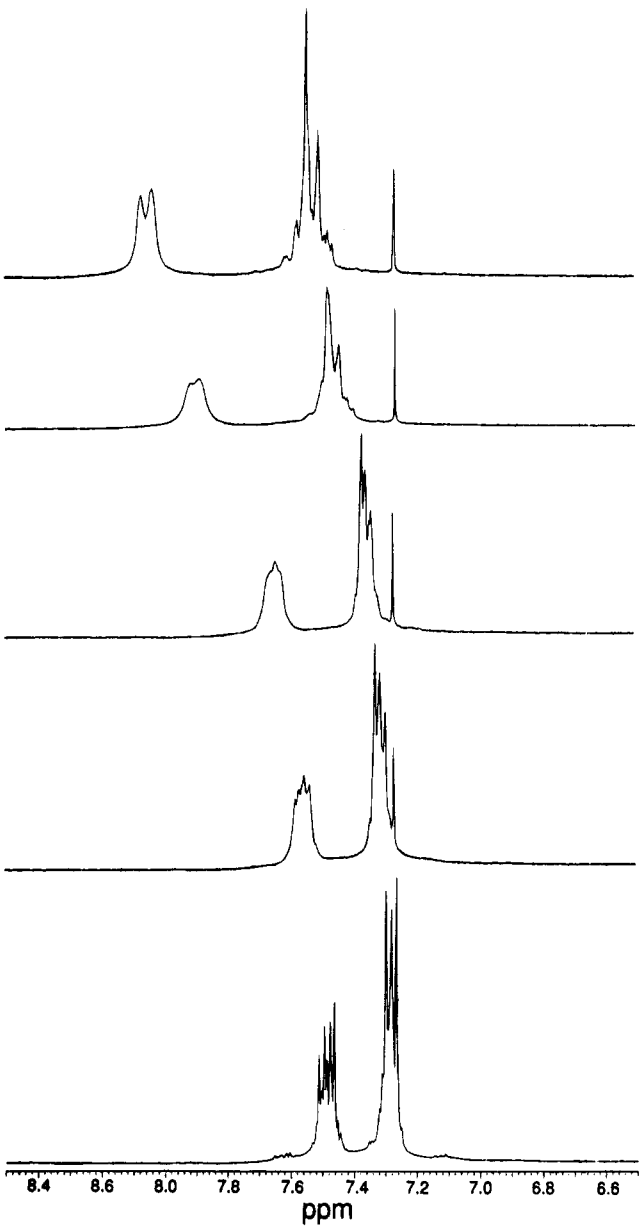

Figure 5. Effects of added tetra-*n*-butylammonium bromide on the ^{1}H NMR spectrum of a 0.01 M $CDCl_3$ solution of **8**. From the top, tetra-*n*-butylammonium bromide concentrations are 0.0, 0.01, 0.02, and 0.05 M. The bottom spectrum is that of diphenyl selenide (**1**) in $CDCl_3$.

found in **3** and **6** with electron-withdrawing π-frameworks do not react with bromine while the Se atom of **1**, which is more electron rich, gives oxidative addition of bromine. In the organotellurium series, all substrates described here react with bromine but the rates of oxidative addition are slower for electron-deficient Te centers, as found in **4**, **5**, and **7**.

The initial fast reaction is followed by one or more slower reactions to give the final products. From the kinetic studies, the initial fast reactions have near-zero values of E_a and $\Delta H^{\ddagger}$ and barriers to reaction are largely entropic. If the fast step were to form an association complex or charge-transfer complex as either an η^1- or η^2-complex, then one would expect small barriers to activation with entropic control. If the middle process observed with **1** and **7** were an ionic dissociation of this complex such as depicted in path C of Scheme 1, then more positive values of E_a and $\Delta H^{\ddagger}$ would be expected with less negative values of $\Delta S^{\ddagger}$ due to the dissociative nature of the process. While such values were found for **7** (E_a = 15.2 kcal mol^{-1}, $\Delta S^{\ddagger}$ = 14.6 kcal mol^{-1}, $\Delta S^{\ddagger}$ = −13 cal mol^{-1} K^{-1}), the limited data make the numbers suggestive rather than conclusive. Kinetic control in the collapse of the ion pairs would generate one mixture of oxidative-addition products (path D of Scheme 1). If the slower reactions that are observed here, with values of E_a and $\Delta H^{\ddagger}$ in the 6.5−8.9 kcal mol^{-1} range and large negative values of $\Delta S^{\ddagger}$, represent the conversion of a kinetic mixture to a thermodynamic mixture, then the Arrhenius and Eyring activation parameters reflect either an ionization pathway as in path D of Scheme 1 or a pseudorotation pathway, as depicted in path E.

The addition of bromine to **13** gives an oxidation product **14**, which is best described as ionic. Although this is a loaded system in the sense that the nitrogen acts as a second electronegative donor ligand, the ionic nature is consistent with steps C and D of Scheme 1. Furthermore, the observations that the addition of bromide to chalcogen(IV) derivatives **8** or **9** leads to the corresponding chalcogen(II) derivatives **1** or **2**, respectively, and that loss of bromine from **8** occurs upon heating suggest that the steps leading to oxidative addition are reversible, that oxidative addition of bromine is an equilibrium process, and that formation of a product mixture under themodynamic control from an initial product distribution under kinetic control is a plausible mechanistic event in these systems.

Experimental Section

Melting points were determined on a Thomas-Hoover melting point apparatus and are uncorrected. ^{1}H NMR and ^{13}C NMR spectra were recorded on a General Electric QE-300 spectrometer or on a Varian Gemini-200 spectrometer. UV−visible−near infrared spectra were recorded on a Perkin-Elmer Lambda 9 spectrophotometer. Infrared spectra were recorded on a Beckman IR 4250 instrument. Microanalyses were performed on a Perkin-Elmer 240 C, H, and N analyzer. Dichloromethane, ethyl acetate, acetonitrile, and carbon tetrachloride were obtained as anhydrous from Aldrich Chemical Co. and were used as received. Distilled water was purified with a Milli-Q water system made by Millipore Corp. to a resistance of 16−17 MΩ cm^{-1} before use. Diphenyl selenide (**1**) and diphenyl telluride (**2**) were obtained from various commercial sources and were distilled prior to use. Selenopyranone **3** and telluropyranones **4** and **5** were prepared according to ref 17. 4-Dicyanomethylidene derivatives **6** and **7** were prepared according to ref 9.

General Procedure for the Oxidative Addition of Bromine on a Preparative Scale. Selenium- or tellurium-containing substrate (2.0 mmol) was dissolved in 10 mL of acetone. A 2.5-mL aliquot of a 1.0 M solution of bromine in carbon tetrachloride was added dropwise, and the resulting solution was stirred 15 min at ambient temperature and was then chilled. The crystalline product was collected by filtration. The crystals were washed with small portions of cold acetone and dried.

For 8: 78%, mp 149−150 °C dec (gas evolution); ^{1}H NMR ($CDCl_3$) δ 8.04 (br d, 4 H, *o*-H), 7.45−7.60 (m, 6 H).

For 9: 75%, mp 198−200 °C; ^{1}H NMR ($CDCl_3$) δ 7.71 (AA′BB′, 4 H, *o*-H), 7.16−7.36 (m, 6 H).

For 10: 71%, mp 224−227 °C (lit.[9] mp 225−227.5 °C); ^{1}H NMR ($CDCl_3$) δ 6.12 (s, 2 H), 1.60 (s, 18 H); IR (KBr) 2960, 2920, 2850, 1615, 1470, 900 cm^{-1}.

(17) Detty, M. R.; Hassett, J. W.; Murray, B. J.; Reynolds, G. A. *Tetrahedron* **1985**, *41*, 4853.

For 11: 79%, mp 209–211.5 °C (lit.[9] mp 208–210 °C); ^{1}H NMR ($CDCl_3$) δ 7.75 (m, 4 H), 7.55 (m, 6 H), 6.45 (s, 2 H); IR (KBr) 3020, 1615, 1585, 1445, 1205, 765 cm^{-1}.

For 12: 70%, mp 207–208 °C (lit.[9] mp 207–208 °C); ^{1}H NMR ($CDCl_3$) δ 6.85 (s, 2 H), 1.63 (s, 18 H); IR (KBr) 2980, 2220, 1620, 1580, 1470, 1360, 1315, 875 cm^{-1}.

For 14: 48%, mp 182–184 °C; ^{1}H NMR (CD_2Cl_2, 303 K) δ 8.58 (br s, 1 H), 7.75 (m, 4 H), 7.67 (t, 1 H, J = 7 Hz), 7.58 (t, 3 H, J = 7 Hz), 7.49 (d, 1 H, J = 7 Hz), 3.87 (br s, 2 H), 2.66 (br s, 6 H); IR (KBr) 1712, 1475, 1462, 1437, 1289, 1055, 1025, 995, 832, 756, 736, 688, 469, 461, 455 cm^{-1}; UV–vis (CH_2Cl_2) [λ_{max}, nm (ϵ)] 324 (5300), 259 (23 400), 253 (26 000). Anal. Calcd for $C_{15}H_{17}Br_2NTe$: C, 36.13; H, 3.44; N, 2.81. Found: C, 35.83; H, 3.64; N, 2.48.

Stopped-Flow Experiments. All stopped-flow experiments were performed on a Sequential DX17 MV stopped-flow spectrometer (Applied Photophysics, Leatherhead, U.K.). All experiments incorporated the instrument in stopped-flow mode only. The sample handling unit was fitted with two drive syringes that are mounted inside a thermostated-bath compartment, which allowed for variable temperature experimentation. The optical-detection cell was set up in the 10-mm path length. First- and second-order curve fitting and rate constants used a Marquardt algorithm[18] based on the routine Curfit.[19] Absorption spectra at indicated time points were calculated through software provided by Applied Photophysics. This consisted of slicing the appropriate time points across a series of kinetic traces (at different wavelengths) and then splining the points of a specific time group. Stock solutions of substrates and bromine at appropriate concentrations described in the text were utilized in the stopped-flow experiments.

Calculation of Activation Parameters. Arrhenius parameters were obtained by plotting ln k against $1/T$, with a slope equal to the energy of activation divided by the gas constant, $-E_a/R$, and an intercept equal to the pre-exponential factor, ln A. Eyring activation parameters were determined using transition-state theory. A plot of R ln $(k/T) + R$ ln (Nh/R) versus $1000/T$ gives a linear slope equal to $-\Delta H^{\ddagger}$ and an intercept of $\Delta S^{\ddagger}$, where N is Avogadro's number, h is Plank's constant, $\Delta H^{\ddagger}$ is the enthalpy of activation, and $\Delta S^{\ddagger}$ is the entropy of activation.

(18) Marquardt, D. W. *J. Soc. Indust. Appl. Mathematics* **1963**, *11*, 431.

(19) Curfit is found in: Bevington, P. R. *Data Reduction and Error Analysis for the Physical Sciences*; McGraw-Hill: New York, 1969.

Crystal Structure Data for 14. The data were collected on an Enraf-Nonius CAD-4 diffractometer in the ω–2θ scan mode to a resolution of 0.80 Å using graphite monochromated Mo Kα radiation. The cell was determined on the diffractometer from the least-squares fitting of the angular settings of 25 reflections well distributed in reciprocal space. Three reference reflections were collected periodically for intensity and orientation control. The Bragg peak profiles were processed using the DREADD data reduction package[20–22] to give the intensity and variance for each reflection. An absorption correction was made by taking a number of ψ scans near χ = 90° and applying a least-squares procedure for modeling an empirical transmission surface by fitting coefficients of an expansion in real spherical harmonics to the multiple ψ scanned reflections.[23] After the appropriate scaling and merging of data, the data were subjected to a Bayesian statistical treatment[24] in order to get a better estimate of the intensities and standard deviations of the weak and unobserved reflections. The structure was solved by direct methods using the SHELXTL package [SHELXTL ver. 4.1., Siemens Analytical X-Ray Instruments, Inc., Madison, WI (1990) and ref 25] and has been refined on F^2 using SHELXL93.[23]

The single-bonded phenyl tended to distort slightly during unconstrained refinement and so was constrained to an ideal geometry. The chemically equivalent *ortho* and *meta* carbons on this phenyl were restrained to have the same anisotropic temperature factors. This procedure seemed to make up for some deficiencies in the absorption correction. The refinement to R_1 of 10% was deemed to be acceptable for such an organometallic compound.

Supplementary Material Available: Tables of anisotropic displacement parameters and hydrogen coordinates with isotropic displacement parameters are found in Tables 7 and 8, respectively, for **14** (2 pages). Ordering information is given on any current masthead page.

OM940282+

(20) Blessing, R. H. *Cryst. Rev.* **1986**, *1*, 3.
(21) Blessing, R. H. *J. Appl. Crystallogr.* **1986**, *19*, 412.
(22) Blessing, R. H. *J. Appl. Crystallogr.* **1989**, *22*, 396.
(23) Sheldrick, G. M. *J. Appl. Crystallogr.*, submitted for publication.
(24) Wilson, K.; French, S. *Acta Crystallogr.* **1978**, *A34*, 517–525.
(25) Sheldrick, G. M. *Acta Crystallogr.* **1990**, *46A*, 467.